# Polarization-independent Fabry–Perot interferometer in a hole-type silicon photonic crystal

Xiyao Chen,[1,*] Deyin Zhao,[3] Zexuan Qiang,[2] Guimin Lin,[1] Hui Li,[2] Yishen Qiu,[2] and Weidong Zhou[3]

[1]Department of Physics and Electronic Information Engineering, Minjiang University, Fuzhou 350108, China

[2]School of Physics and Optoelectronics Technology, Fujian Normal University, Fuzhou 350007, China

[3]Department of Electrical Engineering, NanoFAB Center, University of Texas at Arlington, Arlington, Texas 76019, USA

*Corresponding author: chenxy2628@yahoo.com.cn

Received 6 August 2010; revised 22 September 2010; accepted 24 September 2010; posted 24 September 2010 (Doc. ID 132830); published 18 October 2010

We propose and numerically demonstrate a polarization-independent Fabry–Perot interferometer (PI-FPI) based on the self-collimation effect in a hole-type silicon photonic crystal (PhC). By use of the polarization peak matching method, a resonance frequency of the transverse-electric modes can equal that of the transverse-magnetic modes in the PI-FPI, although the transmission spectra are quite polarization dependent due to birefringence of the PhC. For the operating wavelength of 1550 nm, the PI free spectral range of the PI-FPI is up to 32.3 nm, which nearly covers the whole optical communication C-band window. With its small dimensions, simple structure, and silicon-based material, this PI-FPI may play an important role in photonic integrated circuits. 

*OCIS codes:* 230.5298, 050.2230, 250.5300.

## 1. Introduction

Fabry—Perot interferometers (FPIs) or etalons that belong to a kind of typical and important optical filters, have many applications in optical telecommunications, lasers, and optical spectroscopy [1]. Most of conventional FPIs are made of isotropic materials and, thus, are polarization independent. But the FPIs based on photonic crystals (PhCs) that can be applied in high-density photonic integrated circuits are usually polarization dependent due to large birefringence resulting from the anisotropic structure of the PhCs. On the other hand, the self-collimation (SC) effect is a unique phenomenon that allows diffractionless light propagation in perfect PhCs without "physical" guiding boundaries (e.g., the line-defect waveguide) [2,3]. Self-collimated light beams can also intercross without any cross talk in PhCs as in free space. In addition, the SC effect has a certain tolerance to the surface roughness of PhCs [4]. These properties greatly simplify the structures of PhC devices and thus make them convenient for integration. Various PhC filters based on the SC effect have been theoretically and experimentally demonstrated [4–14]. Recently, some FPIs based on the SC effect have been proposed [10,11]. But they work only for transverse-electric (TE) polarization, which restricts their practical applications. As large birefringence exists in PhCs, it can be anticipated that TE and transverse-magnetic (TM) transmission spectra of a FPI are quite different even in the common SC frequency range. Very recently, we designed a polarization-independent drop filter based on a PhC SC ring resonator, which can drop both TE and TM light channels at the same resonance frequency [12]. It is thus possible to design a PI-FPI with a similar method.

In this paper, we first analyze the PI SC frequency range in a hole-type square-lattice silicon PhC, followed by the structure and characteristics of the FPI based on the SC effect. Then the performance of a PI-FPI is demonstrated. All the characteristics

0003-6935/10/305878-04$15.00/0

are analyzed by using the two-dimensional (2D) finite-difference time-domain (FDTD) numerical technique. Finally, we draw the conclusions.

## 2. Polarization-Independent Self-Collimation Frequency Range

Here we consider a 2D PhC consisting of a square lattice of air holes in silicon (Si) with the dielectric constant $\varepsilon$ of 12.25, as shown in the inset of Fig. 1(c). The radius of the air holes is $r = 0.33a$, where $a$ is the lattice constant. Figures 1(a) and 1(b) show some equal frequency contours (EFCs) of the first photonic band in a quarter of the first Brillouin zone for TE and TM modes, respectively. Dispersion curves along the ΓM direction for two polarizations are also plotted in Fig. 1(c). All are calculated with the plane-wave expansion method.

The direction of the energy flow for light propagation is always perpendicular to the corresponding EFCs [15]. From Figs. 1(a) and 1(b), the EFCs in the frequency range between 0.173 $c/a$ and 0.187 $c/a$ for both TE and TM polarizations are close to straight lines normal to the ΓM direction (where $c$ is the speed of light in vacuum). This indicates that both TE and TM lights in that frequency range can travel without diffraction along the ΓM direction in the PhC, which is the so-called SC effect. This PI SC frequency range is essential for forming PI PhC devices.

As shown in Fig. 1(c), the dispersion relations for two polarizations are different, due to the birefringence nature of the PhC. Within the common SC frequency range between 0.173 $c/a$ and 0.187 $c/a$, both polarization modes have approximately linear dispersion relations:

$$f = (c/2\pi n_e)k + f_0, \tag{1}$$

where $n_e$ is the effective refractive index for SC light, $k$ is the Bloch wave vector, and $f_0$ is a fitting parameter. Best linear fits can result in the following parameters: $n_{e,\mathrm{TE}} = 2.9737$, $f_{0,\mathrm{TE}} = 0.01905\ c/a$ for TE polarization and $n_{e,\mathrm{TM}} = 3.9217, f_{0,\mathrm{TM}} = 0.03804\ c/a$ for TM polarization. It is worth noting that significant birefringence exists with the ratio of the effective refractive indices for the TE and TM modes to be $n_{e,\mathrm{TE}}{:}n_{e,\mathrm{TM}} \approx 3{:}4$.

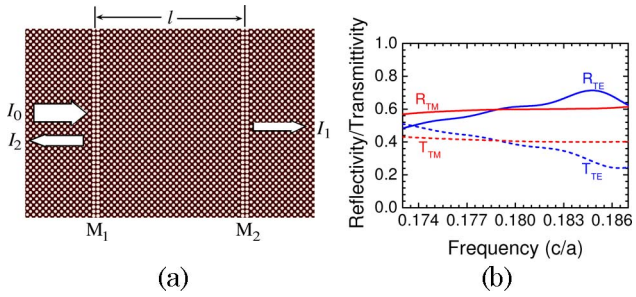


Fig. 2. (Color online) (a) Structure of a FPI consisting of two of the same mirrors ($M_1$ and $M_2$) with spacing $l$ in the hole-type silicon PhC. Each mirror is composed of two parallel rows of air holes with enlarged radius $r_d = 0.396a$. The arrows indicate the propagation directions of the SC light beams. (b) Polarization-dependent reflectivity $R$ and transmittivity $T$ of a mirror in the common SC frequency range.

## 3. Structure and Characteristics of the Fabry–Perot Interferometer

The existence of the PI SC frequency range makes it possible to design SC filters that can work for two polarizations. The structure of a FPI we proposed is shown in Fig. 2(a), which consists of two of the same mirrors $(M_1, M_2)$ in the PhC aforementioned. Each mirror is composed of two parallel rows of inserted air holes with enlarged radius $r_d = 0.396a$, overlapping three rows of air holes along the ΓM direction in the perfect PhC. The length of the resonant cavity of the FPI ($l$) is equal to the spacing between the central lines of the two mirrors. Dependent on the SC effect, narrow light beams in the frequency range 0.173–187 $c/a$ can propagate without diffraction in the PhC along the direction perpendicular to the mirrors.

The reflectivity $R$ and transmittivity $T$ of a mirror over the SC frequency range was first evaluated based on the FDTD simulation method, with the results shown in Fig. 2(b) where $R_{\mathrm{TE}}$ and $T_{\mathrm{TE}}$ are plotted with solid and dashed blue curves respectively, $R_{\mathrm{TM}}$ and $T_{\mathrm{TM}}$ are plotted with solid and dashed red curves, respectively. The mirrors are nearly lossless as $R + T \approx 1$ for both polarizations. It is worth noting that both reflectivity and transmittivity are polarization dependent.

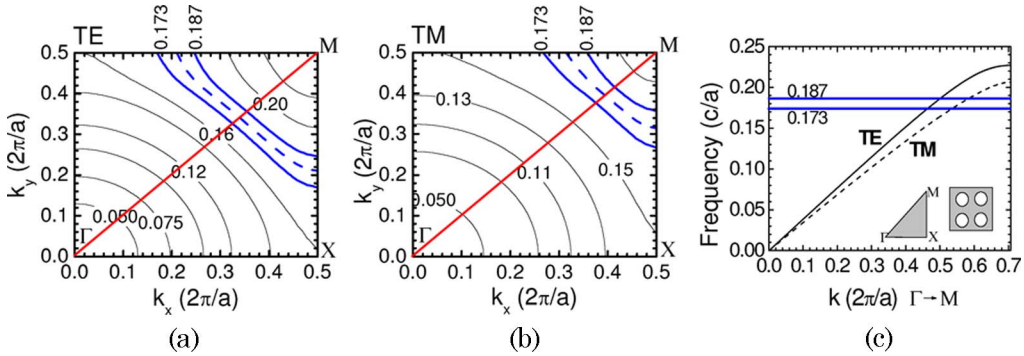


Fig. 1. (Color online) Equal frequency contours of the first band in the wave vector space for (a) TE modes and (b) TM modes. (c) Dispersion curves for two polarizations along the ΓM direction. Inset, the corresponding PhC consists of a square lattice of air holes in silicon. In each figure, the region between the two solid blue curves corresponds to the common SC frequency window.

The theoretical transmission (i.e., $I_1/I_0$) of a FPI can be obtained based on the theory of multiple-beam interference in the following form [1]:

$$\frac{I_1}{I_0} = \frac{1}{1 + [4R/(1-R)^2]\sin^2(\phi/2)}, \tag{2}$$

where $I_0$ and $I_1$ are the intensities of the input and the transmitted light, respectively, and $\phi$ is the phase delay of the SC light after a round trip in the FPI that can be expressed as

$$\phi = 2kl_e = 2k(l + l_p), \tag{3}$$

where $k$ is the Bloch wave vector and $l_e$ is the effective cavity length. $l_p$ is the penetration depth for the SC light at a mirror, which is polarization dependent [12]. From Eq. (2), when the phase delay $\phi$ is equal to the integer multiples of $2\pi$, the transmission reaches the peak value (i.e., $I_1 = I_0$) regardless of the values of the mirror reflectivity $R$.

To verify the theoretical analyses, the numerical transmission spectra of the FPI for TE and TM modes are simulated with the 2D FDTD technique. A Gaussian optical pulse is launched into the FPI from the left side. The input power ($I_0$) and transmitted power ($I_1$) are measured with two power monitors. The transmission spectra for $l = 22\sqrt{2}a$ and $l = 26\sqrt{2}a$ are plotted in Figs. 3(a) and 3(b), respectively, where the solid blue and dashed red curves show the TE and TM transmission spectra, respectively. The ratio of the free spectral ranges (FSRs) for the TE and TM modes is about 4:3 for the same FPI size, which agrees well with the ratio of the effective refractive indices. Most importantly, the peak locations shift at different speeds for the TE and TM modes when the cavity length $l$ changes. This opens up the possibility of matching two peaks for different polarizations by properly selecting the FPI size.

### 4. Design of the Polarization-Independent Fabry–Perot Interferometer

In our early work [12], we utilized the polarization peak matching (PPM) method to design PI drop filters based on a PhC SC ring resonator. Here we also utilize the PPM method to design a PI-FPI. As shown in Fig. 3, TE and TM transmission spectra are quite

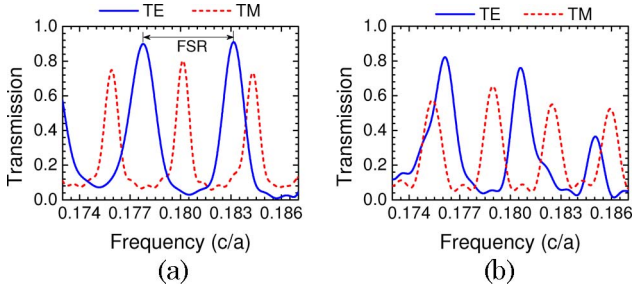


Fig. 3. (Color online) Finite-difference time-domain simulated transmission spectra of the FPI for TE (solid blue curves) and TM (dashed red curves) modes when (a) $l = 22\sqrt{2}a$ and (b) $l = 26\sqrt{2}a$.

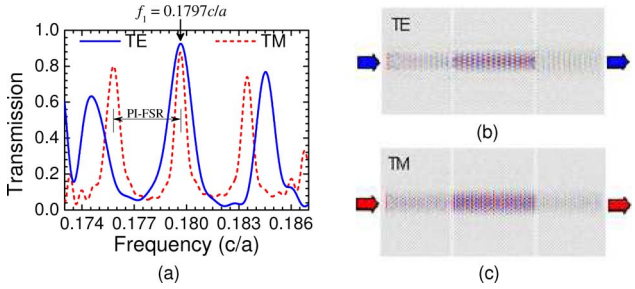


Fig. 4. (Color online) (a) Finite-difference time-domain simulated transmission spectra for both TE (solid blue curves) and TM (dashed red curves) polarizations when $l = 23.974\sqrt{2}a$. Notice the TE peak matches well with the TM peak at $f_1 = 0.1797\ c/a$. (b) Magnetic-field distribution in the PI-FPI for TE polarization at $f_1$. (c) Electric-field distribution in the PI-FPI for TM polarization at $f_1$.

different in terms of peak frequencies and peak spacings. On the other hand, both TE and TM peak frequencies shift when the cavity length $l$ changes. Considering these two factors, we found that a PI-FPI can be formed when a TE peak matches a TM peak, which can be called a PPM case.

It is not difficult to find some PPM cases by changing continuously the cavity length $l$ of the FPI [12]. With the FDTD method, we simulated the transmission spectra for TM and TE polarizations by scanning the cavity length from $l = 15\sqrt{2}a$ to $l = 30\sqrt{2}a$. The results show that the best PPM happens when $l = 23.974\sqrt{2}a$, in which a TE transmission peak matches well with a TM transmission peak at $f_1 = 0.1797\ c/a$ (corresponding wavelength in vacuum $\lambda_1 = c/f_1 = 5.565a$), as shown in Fig. 4(a). The field distribution patterns of SC light at $f_1$ for the TE and TM modes were also simulated as shown in Figs. 4(b) and 4(c), respectively. It can be clearly seen that about 100% intensity of SC light for both polarizations can pass through the interferometer, which means a PI-FPI has been formed.

This PI-FPI can be designed to operate at any frequency according to the scaling law. For example, if the lattice constant $a$ and air hole radius $r$ are equal to 280.1 nm and 92.4 nm, respectively, then the operating wavelength is equal to 1550 nm. The PI-FSR is equal to 32.3 nm, which nearly covers the whole optical communication C-band window.

### 5. Conclusion

At first, we designed a FPI in a hole-type silicon PhC, which can work for both TE and TM polarizations in the common SC frequency window. Then the PPM method was used to form a PI-FPI that can operate at a resonance frequency. Its performance was evaluated with the FDTD simulation technique and good agreements are obtained between the simulation and theory. Although the design of PI-FPIs based on more practical PhC slabs would require three-dimensional (3D) numerical analysis, our 2D results offer a general indication of the expected 3D behavior. As the complete 3D FDTD technique is typically computational time and memory consuming,

here we only discuss the 2D PhC configuration for simplicity. This PI-FPI can work at any frequency by scaling the lattice constant and air hole radius of the PhC simultaneously. For the operating wavelength at 1550 nm, the dimensions of this PI-FPI are about several micrometers and the PI-FSR is up to 32.3 nm, which approximates the whole C-band window of optical communication systems, so it may have applications in high-density photonic integrated circuits.

This work was supported in part by the Natural Science Foundation of Fujian Province of China under grants 2009J01012 and 2009J05140 and by the Program for the Key Teacher in University by the Ministry of Education of China (NCET-04-0615).

### References

1. B. E. A. Saleh and M. C. Teich, *Fundamentals of Photonics* (Wiley, 1991).
2. H. Kosaka, T. Kawashima, A. Tomita, M. Notomi, T. Tamamura, T. Sato, and S. Kawakami, "Self-collimating phenomena in photonic crystals," Appl. Phys. Lett. **74**, 1212–1214 (1999).
3. J. Witzens, M. Loncar, and A. Scherer, "Self-collimation in planar photonic crystals," IEEE J. Sel. Top. Quantum Electron. **8**, 1246–1257 (2002).
4. P. T. Pakich, M. S. Dahlem, S. Tandon, M. Ibanescu, M. Soljacić, G. S. Petrich, J. D. Johnnopolos, L. A. Kolodziejski, and E. P. Ippen, "Achieving centimetre-scale supercollimation in a large-area two-dimensional photonic crystal," Nat. Mater. **5**, 93–96 (2006).
5. L. Wu, M. Mazilu, and T. F. Krauss, "Beam steering in planar-photonic crystals: from superprism to supercollimator," J. Lightwave Technol. **21**, 561–566 (2003).
6. X. Yu and S. Fan, "Bends and splitters for self-collimated beams in photonic crystals," Appl. Phys. Lett. **83**, 3251–3253 (2003).
7. D. W. Prather, S. Shi, J. Murakowski, G. J. Schneider, A. Sharkawy, C. Chen, B. Miao, and R. Martin, "Self-collimation in photonic crystal structures: a new paradigm for applications and device development," J. Phys. D **40**, 2635–2651 (2007).
8. D. Zhao, J. Zhang, P. Yao, X. Jiang, and X. Chen, "Photonic crystal Mach–Zehnder interferometer based on self-collimation," Appl. Phys. Lett. **90**, 231114 (2007).
9. V. Zabelin, L. A. Dunbar, N. L. Thomas, and R. Houdré, "Self-collimating photonic crystal polarization beam splitter," Opt. Lett. **32**, 530–532 (2007).
10. Y. Wang, Y. Qiu, X. Chen, G. Lin, H. Hong, and B. Ni, "Transmission spectrum of Fabry–Perot interferometer based on photonic crystal," Proc. SPIE **6838**, 683804 (2007).
11. R. Iliew, C. Etrich, T. Pertsch, F. Lederer, and K. Staliunas, "Subdiffractive all-photonic crystal Fabry–Perot resonators," Opt. Lett. **33**, 2695–2697 (2008).
12. X. Chen, Z. Qiang, D. Zhao, H. Li, Y. Qiu, W. Yang, and W. Zhou, "Polarization-independent drop filters based on photonic crystal self-collimation ring resonators," Opt. Express **17**, 19808–19813 (2009).
13. T. T. Kim, S. G. Lee, H. Y. Park, J. E. Kim, and C. S. Kee, "Asymmetric Mach–Zehnder filter based on self-collimation phenomenon in two-dimensional photonic crystals," Opt. Express **18**, 5384–5389 (2010).
14. H. M. Nguyen, M. A. Dundar, R. W. van der Heijden, E. W. J. M. van der Drift, H. W. M. Salemink, S. Rogge, and J. Caro, "Compact Mach–Zehnder interferometer based on self-collimation of light in a silicon photonic crystal," Opt. Express **18**, 6437–6446 (2010).
15. P. Yeh, "Electromagnetic propagation in birefringent layered media," J. Opt. Soc. Am. **69**, 742–756 (1979).